Research Paper

Volume : 2 | Issue : 10 | October 2013 • ISSN No 2277 - 8179

Synthesis, Structural and Surface Morphological Characterizations of Tin Dioxide Nanoparticles Via Chemical Route

Physics

KEYWORDS : Tin dioxide, sol-gel, nanoparticles, optical properties, XRD

B. A. Ezekoye	Crstal Growth and Characterization Laboratory, Department of Physics and Astronomy, University of Nigeria.
V. A. Ezekoye	Crstal Growth and Characterization Laboratory, Department of Physics and Astronomy, University of Nigeria.
F. I. Ezema	Crstal Growth and Characterization Laboratory, Department of Physics and Astronomy, University of Nigeria.
P. O. Offor	Department of Metallurgical and Materials Engineering, University of Nigeria.
B. E. Aroh	Crstal Growth and Characterization Laboratory, Department of Physics and Astronomy, University of Nigeria.

ABSTRACT

Tin dioxide (SnO2) nanoparticles were successfully synthesized visa sol-gel technique at 80oC for 1hr. The samples were annealed at 100oC and 300oC for 2hr. The properties of the synthesized samples were investigated using XRD, EDX, SEM, and UV-VIS spectrophotometer. The XRD studies revealed well crystallized tetragonal SnO2 with particle size of 3.0822 nm.

Optical analysis showed that the nanoparticles have wide band gap (3.85 eV). The SnO2 synthesized could find applications in gas sensors, microelectronics and solar cells.

Introduction

Tin dioxide (SnO2) is an important n-type wide-energy-gap semiconductor and has a wide range of applications (Patil, Kajale, Gaikwad & Jain, 2012). It is a white powder having a molecular formula, SnO_2, molar mass 150.709 g/mol with density of 6.95 g/m^3 and high index of refraction of 2.006. It has been studied extensively due to its considerable technological importance and stability (Prodon, Vene, Sevešek, Hudomalji, 1987). SnO2 wires are commonly used as the detecting element in carbon monoxide detectors (Watson). It also is used in sensors of combustible gases where the sensor area is heated to a constant temperature of few degrees Celsius and in the presence of a combustible gas the electrical resistivity drops (Wang et al., 2006 and Dibb A, et al., 2006). By doping SnO2 with cobalt and manganese, gives a material that can be used in high voltage varistors There has been great interest in the gas sensing properties of tin oxide, because it is n-type and is very sensitive to the surroundings. Tin oxide is extensively used as an optically transparent, electrically conducting, and high-band gap material for optoelectronic applications, solar cells, and liquid crystal displays (Moreno, Varela, and. Otero-Dia, 1997). Tin oxide thin films have useful applications due to their high transparency in the visible region and wide energy bandgap.

Several techniques have been used in the synthesis of tin oxide nanoparticles such as spray pyrolysis, precipitation, hydrothermal, gel combustion and sol-gel (Gnanam and Rajendran, 2010;

Patil, Kajale, Gaikwad and Jain, 2011; Patil, Kajale, Gaikwad and Jain, 2012; Patil, Kajale, Ahire, Chavan, Pawar, Shinde, Gaikwad and Jain, 2011; Punnose, etal., 2005). Sol-gel processes have received much attention because of its very good adhesion, and ability to produce thin films with larger area. It is also cheap and easy. In this study, sol-gel technique was successfully used for the synthesis of tin oxide (SnO_2) thin films and crystalline nanoparticles. The samples were investigated for the optical and solid state properties using EDX, SEM, X-ray, TEM and UV-VIS spectrophotometer.

2.0 Experimental Details

2.1 Materials

The primary precursors for the synthesis of SnO2 include: $SnCl_4$.$5H_2$ (stannic chloride pentahydrate), methanol, ammonia (NH_3) (density of 0.88g/cm3 and 27-33% pure), and distilled water. These chemicals were used without further purifications.

2.2 Methods

2.2.1 Preparation of Solution

7g of $SnCl_4$.$5H_2O$ was added to 150ml of methanol to produce a sol. Gel was formed by dropwise addition of ammonia NH_3 (p = 0.88cm3) in the sol to a volume of about 12-13 ml.

Figure 1: Tin oxide nanoparticles on a magnetic stirrer

2.2.2 Deposition of SnO_2 Samples

Microscopic glass slides were used as substrates for the synthesis and were degreased by soaking them in analytical hydrochloric acid (HCl) for 24 hours and washed with detergent, rinsed in distilled water and dried in oven. This degreasing is done to ensure good nucleating sites for the deposition. The prepared bath solution was stirred for 15 minutes, after which the degreased substrates were dipped for 4mins. The substrates were dipped and removed every four (4) minutes, to obtain eight (8) thin film samples. The sample slides was then removed and rinsed. Four of the samples were annealed at 100° C for 1hr, and the rest four annealed at 300°C for 2 hr. One each of the samples from the two sets was further investigated using UV-VIS spectrophotometric analysis.

2.2.3 Preparation of Crystalline Nanoparticles

The prepared gel was removed by filtering and the sample was dried at 80°C for 1hr. The dried samples were then annealed at 300°C for 2hrs, after which it was grinded to powder and then packaged for analysis.

Figure 2: The synthesize crystalline SnO_2 nanopaticles (NPs).

The samples were characterized using powder X-ray diffraction (XRD). The XRD studies were carried out on a XPERT-PRO diffractometer with CuKα radiation with a scan speed of 0.8s and scan step of 0.02 °.

2.2.4 Equation of the reaction

The possible reaction for the process is as follows:

$$SnCl_4 + 4CH_3OH \xrightarrow{H_2O} SnO_2 + 2H_2O + 4CH_3Cl \quad (1)$$

$$Sn^{+4}Cl^{-1} + 4CH_3^{+}(OH)^{-} \longrightarrow Sn^{+4}O^{-2} + 2H^{+2}O^{-2} + 4CH_3^{+}Cl^{-1} \quad (2)$$

$$Sn(s) + 4HNO_3 \xrightarrow{H_2O} SnO_2(s) + 4NO_2(g) + 2H_2O \quad (3)$$

$$SnO_2(2) + 2OH^{-} + 2H_2O(l) \longrightarrow Sn(OH)_6^{2-}(aq) \quad (4)$$

3.0 Results and discussion

3.1 X-ray Diffraction Analysis

Fig 4.1 shows the XRD pattern of annealed tin oxide thin films. From the figure, the film shows diffraction peak intensity range of 20.010 - 79.990 at a wavelength of radiation in order of 1.54060Å. This result indicates that the phase transformation of SnO tetragonal to SnO_2 orthorhombic occurs after annealing at 300°C. The presence of low-intensity peaks points out that besides the predominating polycrystalline-like phase, the grown film contains some amorphous-like (poorer polycrystalline) phases, as well. The average crystalline size was obtained using Debye-Scherrer's equation (Patil et al., 2011):

$$D = \frac{K\lambda}{\beta \cos\theta} \quad (5)$$

where K is shape factor (= 0.94), λ is the wavelength of X-ray used (λ = 1.5418 nm), β is the full width at half maximum, FWHM and θ is the angle of diffraction. The value of crystallite size, D is 3.0822 *nm*.

From Bragg's diffraction law,

$$2d \sin\theta = n\lambda, \quad (6)$$

Where n is the order, θ is Bragg's angle and d is the spacing between planes. The lattice constant 'a' was obtained (Kittel, 1996):

$$d_{dkl} = \frac{a}{\sqrt{h^2 + k^2 + l^2}} \quad (7)$$

where d_{hkl} is the distance between planes, (hkl) is the Miller indices and a is lattice constant. The lattice constant was calculated to be 0.15034 *nm*. The distance between planes d_{hkl} was computed to be 0.56252 *nm*. The crystallographic orientation of the film is (3 2 1). The dislocation density ρ (from Williams's law) and the microstrain are given:

$$\rho = \frac{15\varepsilon}{4aD}, \text{ and } \varepsilon = \frac{\beta}{4\cos\theta},$$

were deduced to be 0.5833 and 0.0505 respectively.

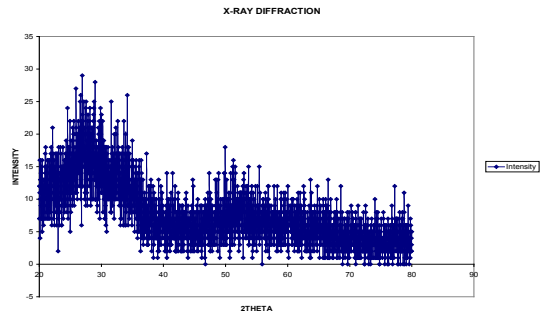

Figure 3: XRD patterns of tin oxide thin films annealed at 300°

3.2 UV-VIS Spectrophotometric analysis

The optical characterization of the tinoxide films using UV-VIS spectrometer are shown Figures 4, 5, and 6. Absorbance, transmittance, reflectance all versus wavelengths shown in Figures 4, 5 and 6 respectively. Figure 7 shows that the band gap for P2 is more than that for P1. This shows that optical band gap increase with annealing. Optical band gap increase with annealing confirms the improvement in the quality of film transparency. Electrical conductivity also shows an increasing trend with annealing.

In Figure 4, the absorbance for film P2 is maxima in the value of 1.058 at 505nm which is in the visible region. In the UV region, the film has an average absorbance in the range of 0.88 to 0.809 within the wavelength of 330nm to 380nm. In the visible region, it has average absorbance of 0.917 to 0.8445 in the wavelength range of 430nm to 690nm. The infrared has average absorbance of 0.7925 to 0.7255 in the wavelength of 815nm to 1100nm.

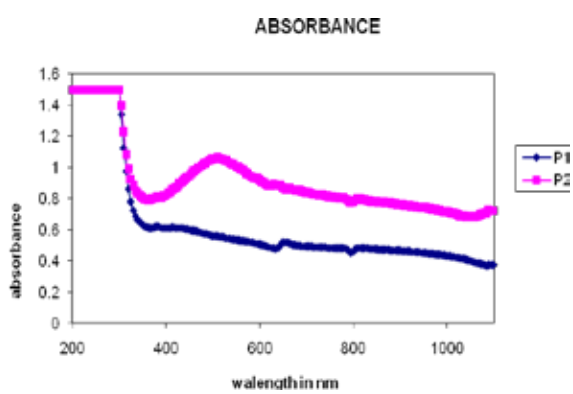

Figure 4: Plot absorbance against wavelength (nm).

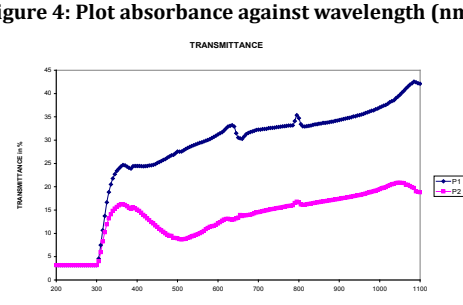

Fig. 5: The transmittance graph against wavelength of SnO_2 Thin film

Volume : 2 | Issue : 10 | October 2013 • ISSN No 2277 - 8179

Plot of transmittance against wavelength, the transmittance shown by Figure 5. The transmittance of tin oxide thin film increased from the near ultraviolet region through the visible region to the near infrared region. However, the film P1 transmits more than P2. This is because transmittance increased with annealing, since P2 was annealed at 300°C. There is noticeable increase in transmittance with value of 33.075 at 630nm and also a peak point of 56.359 at 795nm of sample P1 as compared to that of sample P2 with peak value of 16.5006 at 790nm. The films have relatively low transmittance of 42.218 at 1095 nm. The transmission edge is greater than 650 nm sand shifts toward the higher wavelength. This shows that the films are becoming more transparent and are in a higher wavelength range. From Figure 6 the reflectance is low with P2 being more reflected than P1, though the peak of P2 reflectance and the peak of P1 are common. The reflectance ranges from 0.1351 at 350nm to 0.2023 at 1050nm.

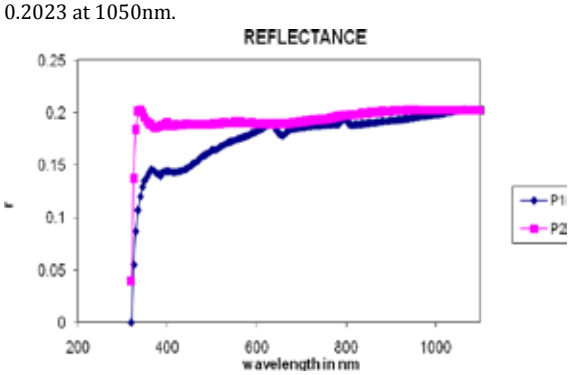

Figure 6: Plot of reflectance against wavelength of SnO_2 thin film

The direct energy band gap of tin oxide depicted in Figure 7 which was obtained from the plot of $(ahv)^2$ against hv (eV).

The energy band gap revealed lies between 3.8e$\pm$0.05V and 3.90 $\pm$0.05eV, approximately 3.60$\pm$0.05eV in agreement with Prodon (2010).

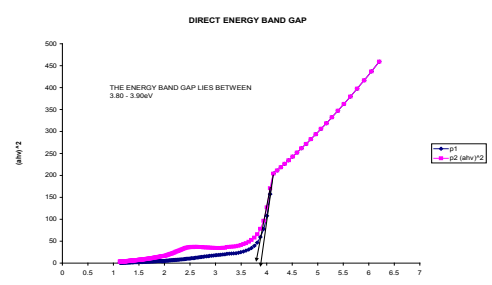

Figure 7: Plot of $(\alpha h\nu)^2$ against photon energy (eV).

3.3 Scanning Electron Microscope Analysis (SEM)

Figures 8, 9 and 10 show the SEM analysis SnO_2 samples with EHT = 20.00kV at different magnifications.

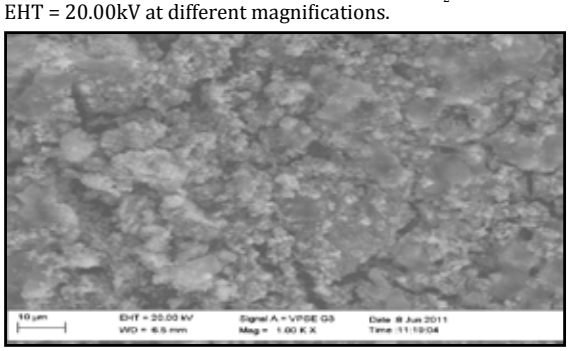

Figure 8: SEM image of SnO_2 thin film at 1000x magnifications.

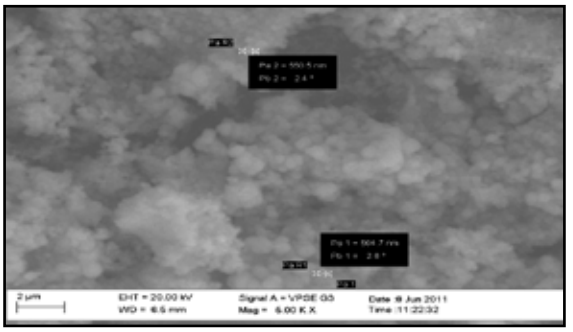

Figure 9: SEM image of SnO_2 at 5000x magnifications

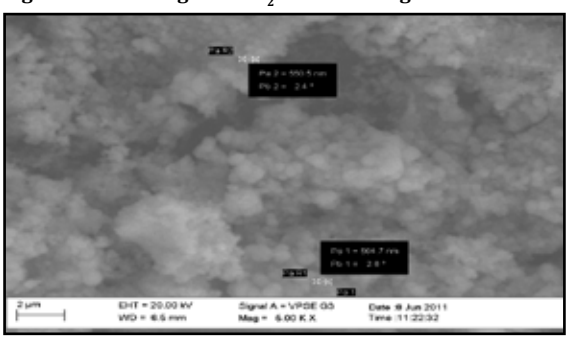

Figure 10: SEM image of SnO_2 at 500x magnifications.

3.4 Energy Dispersive X-ray Analysis

Figure 11 is the EDXA spectrum of the tin oxide sample showing the elemental compositions. The ratio is Sn:O (2:1) showing that sample is rich in thin, [Sn]O[Sn].

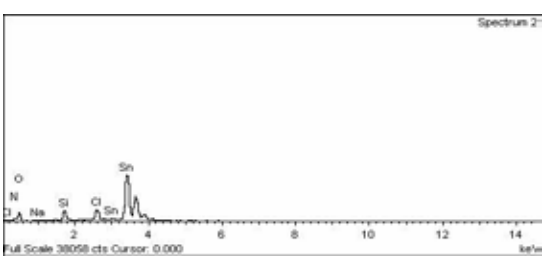

Figure 11: EDX spectrum of tin oxide thin film.

4.0 Conclusion

Tin oxide (SnO_2) nanoparticles were successfully synthesized via sol-gel and chemical bath techiques. The XRD studies showed that the samples were crystalline in nature. The optical characterizations showed wide energy bandgap of 3.58 $\pm$ 0.05 eV. The synthesized nanoparticles could find applications in gas sensors, microelectronics and solar cells.

REFERENCE

Waston, J. The Stannic Oxide Semiconductors Gas Sensor In The Electrical Engineering Handbook 3rd Edition; Sensors Nenoscience Biomedical Engineering And Instruments ed R.C, Dorf CRC Press Taylor and Francis ISBN 0-8493-70346-8. | Wang, Chun-Ming; Wang, Tin-Feng; Su, Wen-Bin (2006.) "Microstructural Auorphology And Electrical Properties Of Copper And Niobium-Doped Tin Dioxide Polycrystalline Varistor: Journal Of The American Ceramic Society 89(8): 2502-2508 Cloi:10.1111/J.1551-2916.2006.01076. | Dibba A. Varela J.A., Longo E. (2006). "Evaluation Of Rare Earth Oxide Doping Sno2(C00.25, Mn0.75) O-Based Vanistor System: Materials Research 9(3):339.-343.doi:10.1590/51516-14392006 000300015. | | Patil, G. E., Kajale, D. D., Gaikwad, V. B., Jain, G. H. "Spray Pyrolysis Deposition of Nano-structured Tin Oxide Thin Films" SRN Nanotechnology, | volume 2012 , 2012, 5 pages. | Prodon, A., Vene, N., Sevešek, F., Hudomalji, M., Thin Solid Films,1987. | | | Kittel, C (1976). Introduction to Solid State Physics. Bristol: Wiley | Gnanam, S., Rajendran, V. (2010). Synthesis of thin oxide nanoparticles by sol-gel process: effects of solvent on optical properties. J Sol Gel Sci Technol. 53: 553-559. | Patil, G.E., Kajale, D. D., Gaikwad, V. B., Jain, G. H. (2011).Nanocrystalline tin oxide thin film as a low level H2S gas sensor. Int. J. Nanosci. 10: 1 | Patil, G. E., Kajale, D. D., Gaikwad, V. B., Jain, G. H. (2012). Preparation and characterization of SnO2 nanoparticles by hydrothermal route. Int. Nano Letters. 2:17. | Patil, G. E., Kajale, D. D., Ahire, P. T., Chavan, D. N., Pawar, N. K., Shinde, S. D.,Gaikwad, V. B., Jain, G. H. (2011). Synthesis, characterization and gas sensingperformance of SnO2 thin films prepared by spray pyrolysis. Bull. Mater. Sci.120: 1. | Punnose, A., Hays, J., Thurber, A., Engelhard, M. H., Kukkadapu, R. K., Wang, C., Shutthanadan, V., and Thevuthasan, S. (2005). "Developing Of High Temperature Ferro Magnetism In Sno2 And Paramagnestism In Sno By Fe Doping: Phys. Rev.B.72(8):054402.doi:10. 1103/phys RevB.72.054402. | Moreno M.S, Varela A. Otero-Diaz L.C (1997) Phys. Rev. | Prodon, A. Vene, N. Sevešek, F. Hudomalji, M. (1987). Thin Solid Films. | |